

Received September 4, 2021, accepted September 13, 2021, date of publication September 22, 2021, date of current version September 30, 2021.

Digital Object Identifier 10.1109/ACCESS.2021.3115045

A Low Cost Front-End Converter With Maximum Power per Ampere for Rooftop Wind Turbines

MEHDI ALEMI-ROSTAMI¹, GHASEM REZAZADEH²,
FARZAD TAHAMI², (Senior Member, IEEE),
AND MOHAMMAD HASAN RAVANJI², (Member, IEEE)

¹Khayam Research Institute (KRI), Ministry of Science, Research, and Technology, Tehran 1465774111, Iran

²Electrical Engineering Department, Sharif University of Technology, Tehran 1458889694, Iran

Corresponding author: Farzad Tahami (tahami@sharif.edu)

ABSTRACT Small Permanent Magnet Synchronous Generators (PMSGs) are widely used in small rooftop wind turbines. In order to inject the electric power generated by the PMSG, into the grid, a back-to-back AC/DC/AC converter is required. In this paper, a low cost with high efficiency converter is proposed for the rectifier stage to obtain the maximum power per ampere of PMSG. This structure based on Discontinuous Conduction Mode Single-Ended Primary Inductor Converter (DCM SEPIC) with a single power electronic switch, proposes a converter which is cost-effective and suitable for the small wind turbine used in residential applications. Furthermore, other advantages of the proposed converter include obtaining maximum power delivered per ampere using a simple control method and reducing the size of converter inductive filter by exploiting the PMSG internal synchronous reactance as part of the filter. Unlike the conventional DCM Boost rectifiers, the proposed converter has a continuous input current, which results in lower PMSG conduction loss. Operation principles and various operating modes of this converter are discussed in detail in this paper and verified by closed-loop simulation and experimental results for a 500W/200V prototype.

INDEX TERMS Micro wind generation, permanent magnet synchronous generator (PMSG), power factor correction (PFC), single-ended primary inductor converter (SEPIC).


I. INTRODUCTION

Global wind turbine market has been increasing rapidly in the past few years and became one of the fastest growing renewable energy sources with a considerable market share in the world [1]–[3]. In recent years, direct-drive wind turbines, i.e. gearless wind turbine systems comprising synchronous generators have gained popularity because of their lower maintenance costs due to the elimination of gearbox failures [4]–[6]. Accordingly, variable-speed wind turbines with Permanent Magnet Synchronous Generators (PMSGs) are the most common solutions for the small-scale wind power plants because of their direct-drive capability, simple construction, and maintenance-free operation [7]–[9]. Wind power micro generation is the use of small wind turbines that convert wind energy into electricity. Roof mounted wind turbine could fully utilize the height of building and the building roof space to harvest energy. Small wind turbines are generally rated at 400W to 1kW and should be made highly affordable to be

suitable for residential, commercial, agricultural, and village electrification uses [10].

The PM wind turbine generator requires a back-to-back power electronic converter to convert the variable-frequency variable-voltage generator power to the fixed-frequency fixed-voltage output compatible with the mains [11]. The front-end converter can be either passive or active. With the active front-end converter, the power factor of the rectifier can be improved which leads to input current reduction, and consequently the conduction loss of the PMSG is reduced [9]. In addition, it can reduce the total harmonic distortion (THD) of the input current, which allows shrinking the input filter size [12].

Active rectifiers are usually categorized into two different types [13], [14]: 1) Phase Modular Rectifier (PMR) consisting of three single-phase PFCs with individual control for each phase, and 2) Direct Three-phase Rectifier (DTR) consisting of a single three-phase transformerless structure. DTRs are remarkable solution for small wind power application compared to the PMRs in terms of component count. Regardless of the rectifier structure, it can be controlled in two different operation modes: continuous conduction mode

The associate editor coordinating the review of this manuscript and approving it for publication was Ahmed F. Zobaa .

(CCM) and Discontinuous conduction mode (DCM) [15]. Generally, DCM has simpler control strategy and circuitry for controlling the rectifiers [16], which is a better choice for small wind power applications.

The three-phase single-switch DCM boost can be a common choice. Although three-phase single-switch DCM Boost seems so simple and efficient, it has a main drawback of discontinuous input current waveform that makes it unsuitable for PMSG applications [17]. The discontinuous input current increases the amplitude and THD of the PMSG current, which can be harmful to the generator [9]. The generator internal voltage waveform is close to sinusoidal, so current harmonics produce no effect on the real power transferred to the converter. Contrarily, the current harmonics flowing through the generator stator windings will induce additional loss which reduces the efficiency and causes temperature rise in the windings. The temperature rise reduces the life span of the PMSG and premature aging of the insulation. To solve this problem, a DCM SEPIC rectifier is proposed in this paper.

The operation principles of the single-phase DCM SEPIC is described in [18]. In [19], a single-stage single-switch soft-switching three-phase DCM SEPIC converter is introduced and analyzed with five different operation modes. In [20], a modified bridgeless SEPIC rectifier with extended gain for universal input voltage applications is presented, which works in DCM condition. Phase modular configuration of the three-phase DCM SEPIC is investigated in [21]. In addition, there are some other valuable research works on different single-phase DCM SEPIC structures such as the single-switch, double-switch, voltage-doubler, and double output in literature [22]–[25].

The proposed configuration provides the following features:

- Low-cost single switch structure,
- Simple control strategy in DCM,
- Soft switching operation without using any auxiliary resonance circuit,
- Simplicity of analyzing the operation modes,
- High efficiency due to using PFC, soft switching, and low component count,
- Easy manufacturing due to low component count and simple control circuitry,
- Continuous input current waveform with low THD value,

When a SEPIC DCM converter operates at a constant switch duty cycle, the input current approximately follows the input voltage [18]. The DCM effective resistance is an approximation of the emulated resistance of the DCM SEPIC rectifier. As the effective synchronous inductance of the machine coincides with the SEPIC input inductor, the current follows the internal voltage of the machine. As a result, the overall PMSG current is reduced even more.

The proposed DCM SEPIC rectifier is designed for a 500W rooftop wind turbine generator. The converter is analytically modelled using the single-phase equivalent circuit, and then the simulation results are obtained to verify the analytical

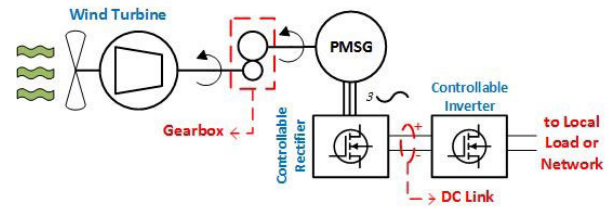


FIGURE 1. Structure of the case study PMSG-based wind turbine generator system including: wind turbine, gearbox, PMSG, and the interface converter (rectifier, DC link and inverter).

TABLE 1. Wind turbine characteristics (considering the gearbox).

Quantity	SYMBOL	UNIT	Value
Nominal wind speed	V_{nom}	m/sec	12
Cut-in wind speed	V_{cut-in}	m/sec	5
Maximum rotational speed	ω_{max}	rpm	300
Minimum rotational speed	ω_{min}	rpm	125
Maximum delivered power	P_{max}	W	500
Minimum delivered power	P_{min}	W	36
Shaft maximum output torque	T_{max}	N.m	15.9
Shaft minimum output torque	T_{min}	N.m	2.8

TABLE 2. PMSG Main characteristics.

Quantity	SYMBOL	UNIT	Value
Rated power	P_{nom}	W	500
Phase number	m	-	3
Shaft rated rotational speed	ω_{nom}	rpm	300
Pole pair number	P	-	10
Nominal operation frequency	f	Hz	50
Rated output phase voltage	E_{nom}	V	44
Total generator weight	M_{tot}	kg	13.1

results. The accuracy of the analytical and simulation results is verified by experimental results.

II. PMSG-BASED WIND POWER SYSTEM

In this section, a typical wind turbine generator for small power applications, including a wind turbine, a gearbox, a permanent magnet synchronous generator and an interface converter, is considered to harvest and convert the wind power to the electrical power. Fig. 1 illustrates the system configuration. In this system, the interface converter is employed to regulate the voltage and current waveforms to comply with the load/mains requirements. Characteristics of the considered wind turbine in this study is given in Table 1. These parameters are essential for determining the PMSG's operating speed and power ranges [26].

PMSG is the most common choice for the generator in small wind power systems. The main characteristics of the examined PMSG are listed in Table 2. Considering the PMSG speed range, the PMSG output frequency varies in the range of 25Hz to 50Hz and the output voltage varies from 22V to 44V. Variations of the generator variables are depicted in Fig. 2 for different wind speeds.

III. SINGLE-SWITCH THREE-PHASE DCM SEPIC WITH PFC

In this section, exploiting the PMSG internal synchronous inductance as the SEPIC input inductance is investigated.

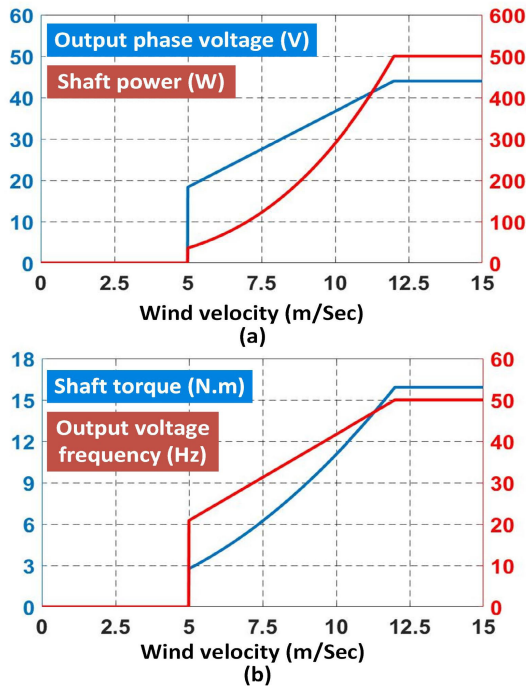


FIGURE 2. PMSG output performance variables for different wind speeds: (a) output phase voltage and shaft power, (b) shaft torque and output voltage frequency.

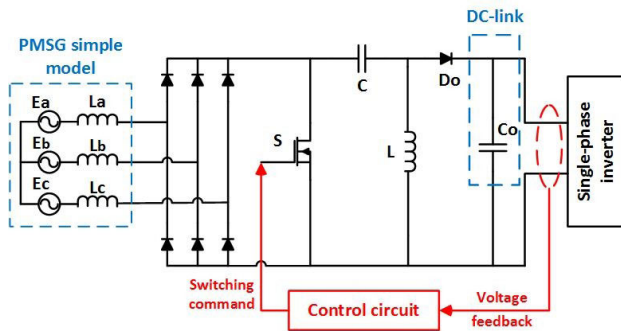


FIGURE 3. Single-switch three-phase DCM SEPIC rectifier.

Then, using the single-phase equivalent circuit model, the converter operation modes are studied for one switching period. Fig. 3 depicts the single-switch three-phase SEPIC rectifier as the active front-end converter. The active rectifier allows to obtain sinusoidal currents in phase with the generator voltage. For this purpose the converter is controlled as a power factor correction (PFC) rectifier.

A. MAXIMUM POWER PER AMPERE

In the conventional PFC method for the rectifier stage, generator terminal is the target point for power factor correction, i.e., the PFC reference point is the generator terminal voltage. The phasor diagram of employing the conventional PFC method is presented in Fig.4.

Unlike the conventional PFC method, in this paper, the PFC concept is used to maximize the power factor out of the PMSG internal voltage (Fig.4 c). It is worth mentioning

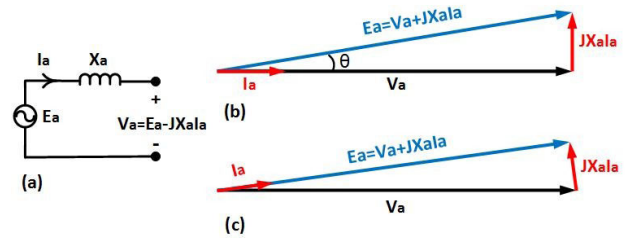


FIGURE 4. Maximum power per ampere method vs. conventional PFC: (a) simple PMSG model, (b) conventional PFC method, and (c) maximum power per ampere.

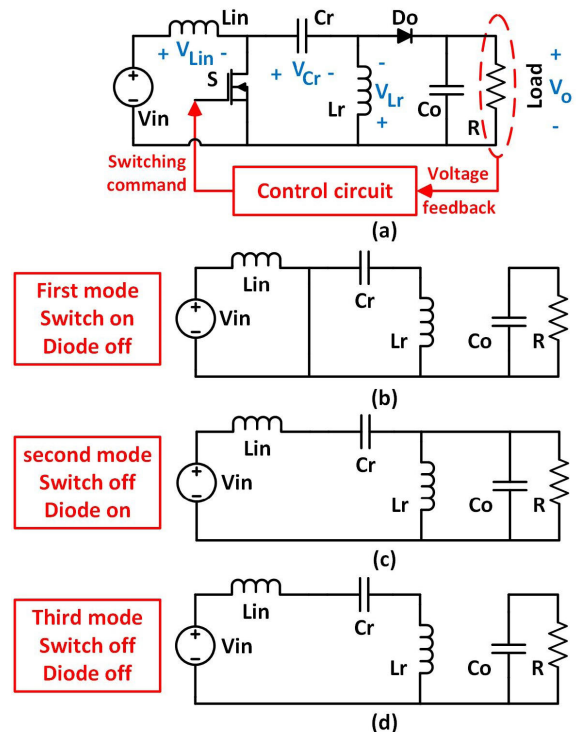


FIGURE 5. DCM SEPIC single-phase equivalent model and its operation modes: (a) single-phase equivalent model, (b) first operation mode, (c) second operation mode, (d) third operation mode.

that in the proposed maximum power per ampere method, since the control method has targeted the PMSG internal voltage, its synchronous reactance can be considered as the converter input inductance, which is beneficial because of rectifier size and manufacturing cost.

B. OPERATION PRINCIPLES

The operation principles of the proposed single-switch three-phase DCM SEPIC can be explained using its equivalent single-phase model [18] depicted in Fig.5, in which the rectifier input voltage and input inductance can be obtained as follows [19]:

$$V_{in} = \frac{3\sqrt{6}}{\pi} E_a, \quad L_{in} = \frac{3}{2} L_a \quad (1)$$

where E_a and L_a denote the PMSG internal phase voltage and synchronous reactance. [9]. Actually, V_{in} and L_{in} are

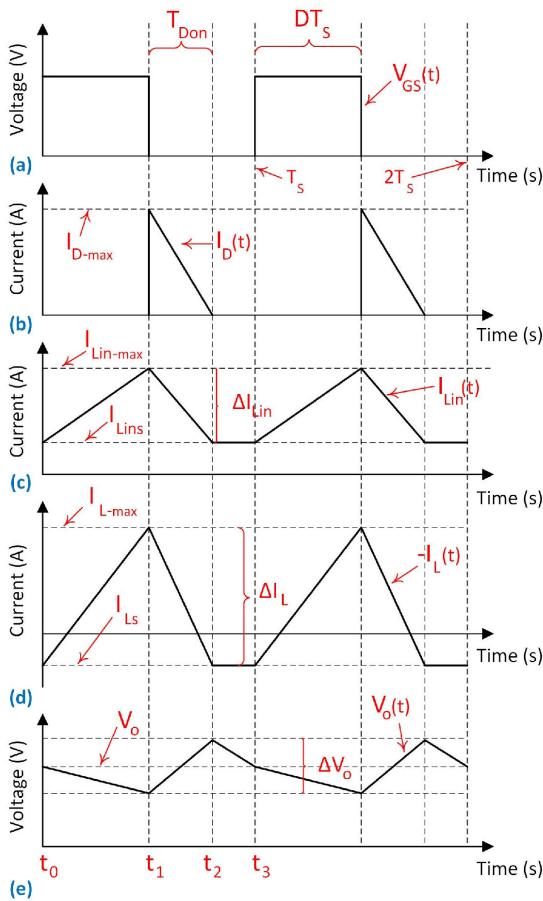


FIGURE 6. Theoretical key waveforms of the proposed DCM SEPIC with three operation modes in each switching period: (a) gate-source voltage, (b) output diode current, (c) the input inductance current, (d) the second inductance current, and (e) output voltage.

representing the rectified voltage and the equivalent of the inductance of the machine reflected to the right side of the three-phase bridge rectifier in Fig. 3.

The three operation modes of the utilized DCM SEPIC and its key voltage and current waveforms are presented in Fig.5 and Fig.6, respectively. Considering these figures, the DCM SEPIC operation principles can be described as follows:

First mode [t_0, t_1]: this mode starts with turning the switch on and ends by turning it off, which results in the mode duration equals to DT_s (see Fig.5. b). In this mode, the input inductance current (i_{Lin}) is obtained as follows [18]:

$$i_{Lin} = \frac{V_{in}}{L_{in}}t + I_{Lins}, \quad \Delta I_{Lin} = \frac{V_{in}}{L_{in}}DT_s \quad (2)$$

where I_{Lins} and ΔI_{Lin} denote the initial and ripple values of the input inductance current, respectively. The current for the other inductance is obtained as follows [18]:

$$i_L = \frac{V_o}{L}t + I_{Ls}, \quad \Delta I_L = \frac{V_o}{L}DT_s \quad (3)$$

where I_{Ls} and ΔI_L denote the initial and ripple current values of the second inductance (L), respectively. In this mode, diode

D_o is off and capacitor C_o supplies the required output power, while the DC link voltage V_o is decreasing. It should be noted that by operating in discontinuous conduction mode, *zero-current turn-ON* of the switch is acquired by the converter, which is favorable.

Second mode [t_1, t_2]: at the beginning of this mode, diode D_o turns on. Second mode ends when the second inductance current reaches to the input inductance current and the output diode turns off. Therefore, the diode turning off occurs in ZCS mode with soft-switching condition. In this mode, the output diode current supplies the required output power and also charges the output capacitor. The currents of both inductances are calculated as follows [18]:

$$i_{Lin} = \frac{V_{in}}{L_{in}}DT_s + I_{Lins} - \frac{V_o}{L_{in}}t \quad (4)$$

$$i_L = \frac{V_o}{L}DT_s + I_{Ls} - \frac{V_o}{L}t \quad (5)$$

Third mode [t_2, t_3]: The output capacitor supplies the required output power, because the output diode is off. The inductances currents are constant without any change in this mode [18]:

$$i_{Lin} = \frac{V_{in}}{L_{in}}DT_s + I_{Lins} - \frac{V_o}{L_{in}}T_{Don} \quad (6)$$

$$i_L = \frac{V_o}{L}DT_s + I_{Ls} - \frac{V_o}{L}T_{Don} \quad (7)$$

where T_{Don} denotes the time period that output diode is on. All the described behaviors of the converter in these three modes are shown in Fig. 6. In the first mode (S_{on}, D_{off}), the voltage across each inductor is positive causing the current through it increases linearly. The output voltage decreases as the output capacitor is discharged by the load current. In the second mode (S_{off}, D_{on}), the current of both inductors decreases linearly since negative voltage is applied to each inductor. On the other hand, the output capacitor is charged and the output voltage increases. In the third mode (S_{off}, D_{off}), the sum of voltages applied to the inductors are zero, thus the values of current remain unchanged. The output voltage is decreased since the output capacitor is discharged by the load current.

IV. DESIGN AND CONTROL OF THE SEPIC DCM PFC

Considering the PMSG operating conditions described in the previous section, the PFC rectifier is optimally designed and an appropriate control circuit is provided for the DCM SEPIC in this section. In this regard, the converter is designed so that it only operates in DCM, which subsequently corrects the input power factor inherently, and the control system only regulates the output power. Converter design is carried out to satisfy the required specifications provided in Table 3.

A. CONVERTER DESIGN

To design the converter, the component value should force the converter to stay in DCM in all operation situations. To achieve this goal, the output diode current must reach

to zero before the switching period ends. In other words, T_{off} must be greater than zero for all operation conditions. The worst operation condition occurs when the input voltage has its peak value. Accordingly, the converter should be designed so that $T_{off} > 0$ [15], which results in the following criterion for the switching duty cycle D [15]:

$$T_{Don} + DT_s < T_s \rightarrow D < \frac{M}{M + 1}, \quad M = \frac{V_o}{V_{in}} \quad (8)$$

where M is the converter voltage gain. Thus, the duty cycle for the critical mode (DCM boundary) can be calculated as follows [18]:

$$D_{cr} = M \sqrt{\frac{2L_{eq-cr}}{RT_s}}, \quad L_{eq} = \frac{L_{in}L}{L_{in} + L} \quad (9)$$

where L_{eq} is defined as the equivalent inductance of the converter, L_{eq-cr} denotes the critical inductance of the equivalent circuit at the DCM boundary condition and R is the load resistance. Substituting (8) in (9) yields [18]:

$$L_{eq} < \frac{RT_s}{2(M + 1)^2} \quad (10)$$

As expressed earlier, the value of L_{in} is determined considering the PMSG synchronous inductance; therefore, the value of L can be calculated using (10).

When a conventional SEPIC converter operates as a PFC, the voltage of the capacitor C is under the following two conflicting constraints: 1) to present a nearly constant value within a switching period and 2) to follow the input voltage profile within a line period [18]. Therefore, it can be calculated as follows [18]:

$$C = \frac{1}{\omega^2(L_{in} + L)} \omega_L < \omega < \omega_s \quad (11)$$

where ω , ω_L and ω_s are the design, line oscillation, and switching frequencies in rad/sec, respectively.

Furthermore, the output capacitor affects the output voltage ripple and can be designed considering the allowable output voltage ripple (ΔV_o), as follows [18]:

$$C_o \geq \frac{V_o(T_s - T_{Don})}{R \cdot \Delta V_o} \quad (12)$$

Following the above design rules, the obtained DCM SEPIC parameters are reported in Table 3 for the aforementioned small wind turbine application.

B. CONTROL SYSTEM

By operating in DCM and using the internal inductances of the generator as the converter components, the power factor value is high between the generator current and the generator internal voltage source without using any additional control loop. In other word, the maximum power per ampere method is achieved inherently in the proposed converter by designing the converter appropriately. Thus, the control system only includes a simple voltage control loop, which regulates the output voltage to its reference value. Accordingly, the control system scheme proposed for the DCM SEPIC is shown

TABLE 3. Designed DCM SEPIC specifications.

Quantity	SYMBOL	UNIT	Value	Size (mm)
Rated input power	P_{in}	W	500	-
Rated input voltage	V_{in}	V	103	-
Rated input current	I_{in}	A	4.85	-
Rated frequency	f	Hz	50	-
Rated output voltage	V_o	V	200	-
Switching frequency	f_s	kHz	50	-
Input inductance	L_{in}	mH	7.5	- ⁽¹⁾
Inductance	L	μ H	50	25×25×10
Capacitor	C	nF	300	10×8×5 ⁽²⁾
Output capacitor	C_o	μ F	200	25×12×12 ⁽³⁾

⁽¹⁾ Equivalent inductance for the PMSG internal inductances

⁽²⁾ Three capacitors with this size are used

⁽³⁾ Two capacitors with this size are used

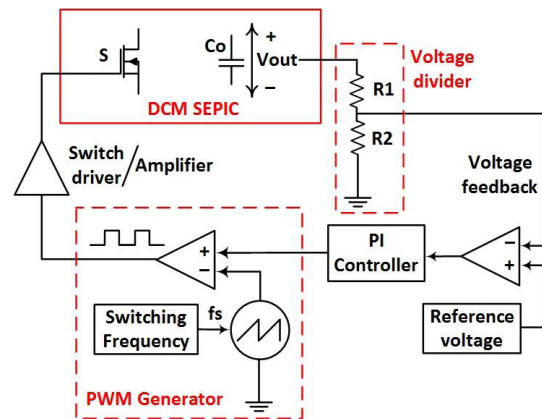


FIGURE 7. Proposed control scheme for the designed DCM SEPIC.

in Fig. 7. In the depicted control system, the non-isolated voltage feedback signal (generated by resistance voltage divider) is compared with the reference voltage signal. To generate the command signal, the result of this comparison passes through the proportional-integral controller. The PWM generator and switch driver are used to convert the command signal to an acceptable gate signal for the switch.

V. SIMULATION AND EXPERIMENTAL RESULTS

A. SIMULATION RESULTS

To validate the analytical results, the proposed DCM SEPIC converter is simulated using PSIM software. Fig. 8 shows the simulation results for the key waveforms of the proposed SEPIC rectifier. As shown, the rectifier operates properly and the operating principles comply with the analytical results. Considering these simulation results, the switch starts in ZCS mode with soft-switching condition, which enhances the converter overall efficiency. In addition, the diode current reaches zero at the end of each switching period, which confirms the DCM operation of the rectifier.

Fig. 9 shows the input voltage and currents waveforms. As shown in Fig.9 (a), the power factor between the internal voltage and its related current is high (96.08%). The phase current is equal to 3.81 A. Therefore, reducing the input inductance component of the DCM SEPIC by replacing PMSG phase inductance as well as using the maximum power per ampere decreases the phase current, which enhances the

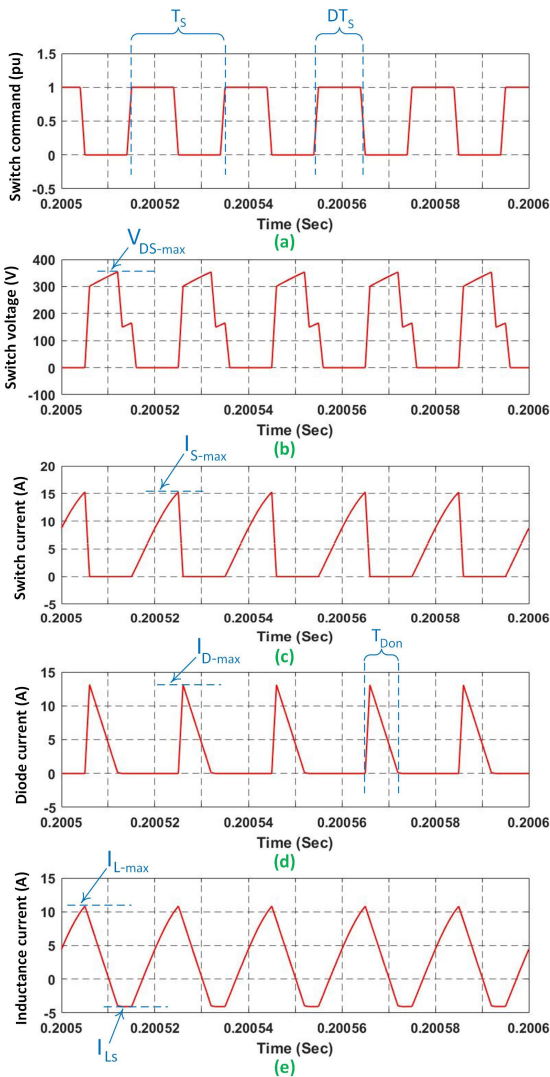


FIGURE 8. Simulation results for the key waveforms of the proposed DCM SEPIC rectifier: (a) switching command signal, (b) drain-source voltage, (c) switch current, (d) diode current, (e) inductance L current.

efficiency. Fig. 9 (b) shows the three-phase input current. The non-symmetrical current waveforms are due to small variation of the emulated input resistance of the converter. The voltage controller should have sufficiently small loop gain at harmonics of the ac line frequency, so that variations in emulated input resistance; R_e , are much slower than the ac line frequency. The low bandwidth of the voltage loop will cause ripple component at the output voltage which in turn causes the variation of the emulated resistance.

On the other hand, by using the MPPA method for the tested PMSG, the required current to deliver 500W reduces by 3.5% compared to the conventional PFC method and consequently the PMSG conductive loss decreases 7.1%. Fig. 10 shows the simulation result for harmonic content of the input current. As can be seen the amplitude of higher order harmonics are quite low showing a THD of 8.5%, which indicates successful operation of the converter.

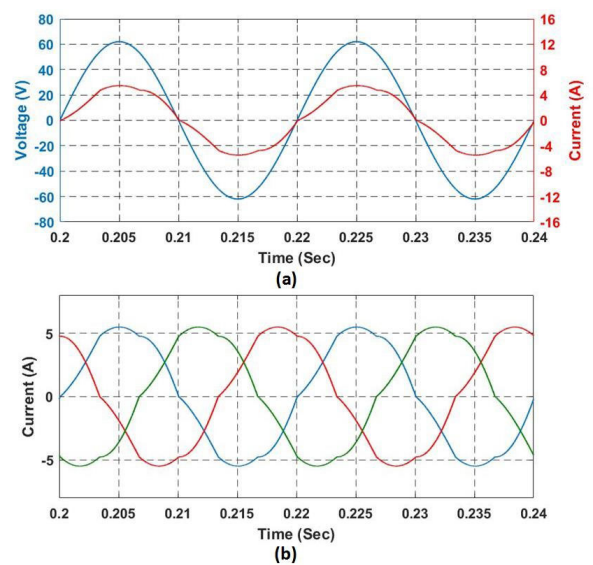


FIGURE 9. Simulation results for the input waveforms of the proposed SEPIC rectifier: (a) The internal voltage (calculated based on measured terminal voltage and current) and the current of one phase of the PMSG, and (b) The current waveforms of the three input phases.

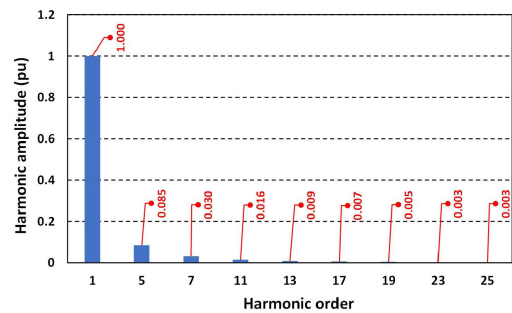


FIGURE 10. Simulation results for harmonic content of the input current.

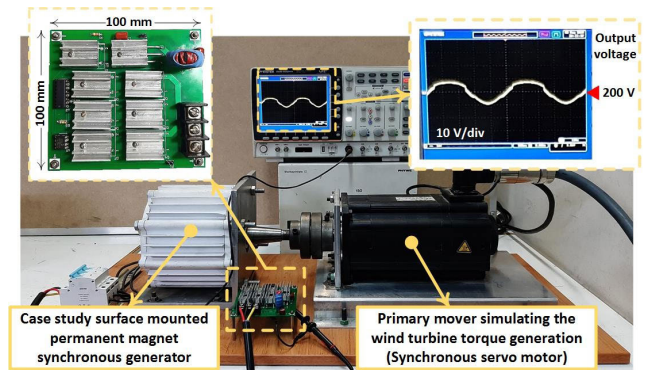


FIGURE 11. Experimental test setup including: Primary mover, permanent magnet synchronous motor, and implemented proposed SEPIC DCM.

B. EXPERIMENTAL RESULTS

The proposed SEPIC converter is implemented (Fig. 11) and the experimental test results are obtained using a test setup. In the utilized test setup, a prime mover as a torque generator is employed, which is an electrical AC motor to emulate the wind turbine behavior. The under-study PMSG is coupled with the prime mover to convert the mechanical

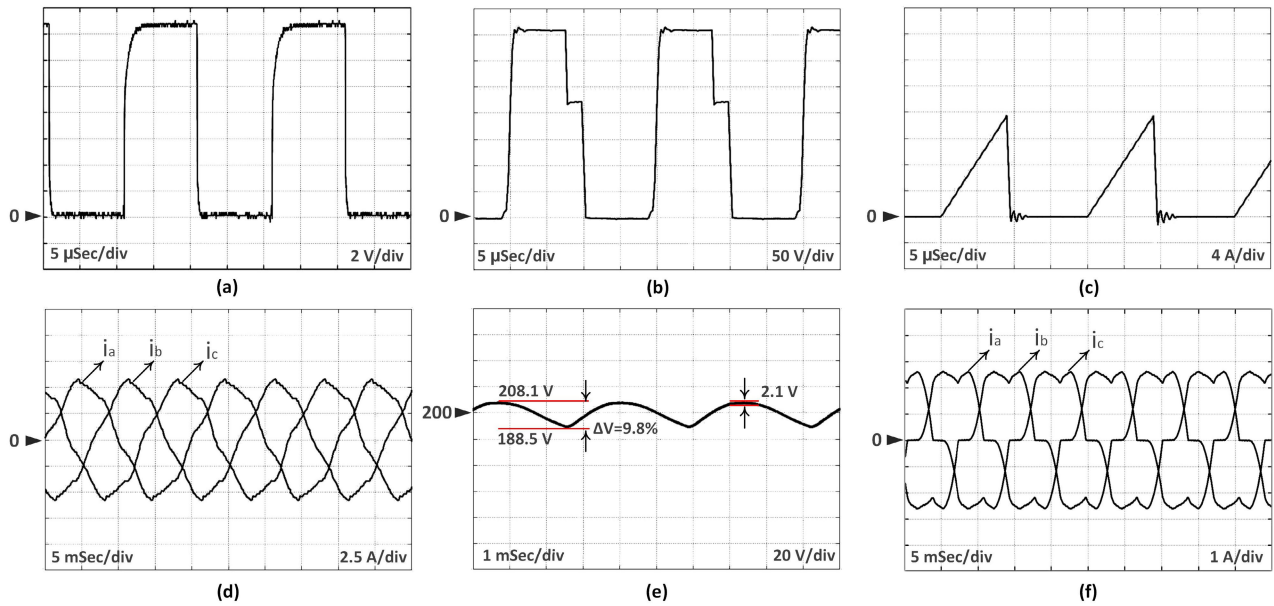


FIGURE 12. Experimental results for the implemented proposed DCM SEPIC rectifier: 1) at the rated condition: (a) gate-source voltage, (b) drain-source voltage, (c) switch current, (d) three-phase input currents waveforms, and (e) output voltage, and 2) at 200 W output power: (f) three-phase input currents waveforms.

power to the electrical power. Also, a variable resistance load is used to change the system load power. The experimental results of the implemented SEPIC DCM are illustrated in Fig. 12. The switch voltage and the current waveforms are completely compatible with the analytical and simulation results. As shown in Fig. 12 (b), the switch current starts smoothly from zero, which verifies the expected ZCS mode soft switching as an advantage of the proposed DCM SEPIC converter, provided without using any auxiliary circuit. The output voltage is successfully set on 200 V with the voltage ripple less than 10%. In addition, the input current waveforms for all three phases are in continuous conduction mode, which reduces the generator conduction losses. There is a symmetrical 120° phase shift between each two different phases; therefore, the converter works under the maximum power per ampere mode with high power factor from the generator internal voltage point of view, as expected.

The experimental results in Fig. 12 agree well with the simulation results shown in figures 8 and 9. From the experimental results one can see that the switch peak voltage and current at the rated condition are 358.9 V and 15.6 A respectively. These values are 360.1 V and 15.2 A from the results obtained by simulation. The input current waveform of the converter also closely matches the simulation results. From the experimental results it can be seen that the input current is 3.86 A(rms) with a THD value of 9.1%. The corresponding values from simulations are 3.81 A(rms) and 8.5% respectively. Therefore, the authenticity of the simulation results and the modeling is validated accurately by the experiments.

C. DIFFERENT OPERATION CONDITIONS

The PMSG internal voltage cannot be measured directly; therefore, the converter efficiency and the PMSG internal

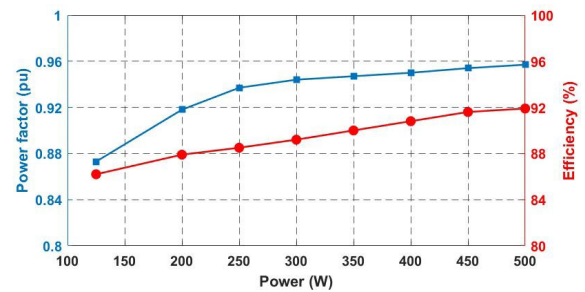


FIGURE 13. Calculated efficiency and power factor based on the measured variables for the three-phase single switch DCM SEPIC.

power factor should be calculated using the measured variables. On the other hand, to investigate the effect of wind speed variations, the designed converter performance should be tested in different operation conditions as shown in Fig. 2. In this regard, the converter should remain in DCM during wind speed variations to keep the power factor in an acceptable range. Fig. 13 shows the converter power factor and efficiency values calculated in different operation conditions. One can see that the converter operates properly and has acceptable performance for a wide range of wind speed variations.

VI. COMPARISON

Four different cases are studied to show the effectiveness of the proposed SEPIC converter with the maximum power per ampere control strategy compared to the other conventional PFC rectifiers:

- **Case 1:** conventional six-switch full-bridge with active PFC control strategy,
- **Case 2:** conventional DCM Boost rectifier with DCM PFC control strategy,

TABLE 4. Simulation results for the performances of the four studied converters (cases 1-4).

Quantity	UNI τ	Different studied cases			
		1	2	3	4
Rated input power	W	500	500	500	500
Rated phase voltage	V	44	44	44	44
Rated frequency	Hz	50	50	50	50
Rated output voltage	V	200	200	200	200
Switching frequency	kHz	50	50	50	50
Continuous input current	-	Y	N	Y	Y
Removing input inductance	-	-	N	N	Y
Simple control circuit	-	N	Y	Y	Y
Rated input current	A	3.80	3.93	3.94	3.81
Peak value of input current waveform	A	5.72	11.08	5.42	5.24
Power factor over internal source	-	0.964	0.931	0.929	0.961
Power factor cross terminal	-	0.997	0.962	0.961	0.994
Switch number	-	6	1	1	1
Switch maximum current	A	5.72	24.21	15.53	15.02
Switch maximum voltage	V	200	200	358	351
Converter dimensions	cm	15×15	10×10	10×10	10×10
Input current THD	%	3.2	104.8	9.3	8.5
Generator loss*	p.u.	0.994	1.064	1.069	1
Efficiency*	%	90.72	89.69	90.87	92.15
Cost of main components	\$	26.6	16.9	20.8	17.8

* Calculated with the same On-delay, Off-delay, rising, and falling times for the all the switches in all cases.

- **Case 3:** DCM SEPIC with DCM PFC control strategy,
- **Case 4:** DCM SEPIC with DCM maximum power per ampere control strategy.

These converters are designed to operate under identical operating conditions as shown in Table 2. All the four converters are designed to have less than 10% voltage ripple. Fig. 12 (e) shows that the designed converter meets this requirement. The same output power and full-load voltage are considered for the PMSG in all four-cases. The converters are simulated using the PSIM software and the results are reported in Table 4. Based on the obtained results, a comparison between the proposed converter and the other conventional converters has been made. The control system cost is not taken into account as it highly depends on the control strategy. Obviously, the converters with the simple control strategy (DCM BOOST and DCM SEPIC) can use low cost controllers. For the power circuit, only the cost of main components including switches, diodes, inductances, and capacitors have been considered.

The comparison between the presented converter (case 4) and the other cases can be summarized as follows:

A. CASE 4 vs. CASE 1

The DCM SEPIC with MPPA control strategy provides input characteristics almost as good as the six-switch full-bridge converter from the terminal point of view. However, compared to the case 1, the proposed converter has simpler control strategy and lower power components cost. Case 1 uses more switches with considerably lower current rating compared to the proposed single-switch DCM SEPIC. It can be concluded that the proposed converter is simpler with lower

manufacturing cost compared to the conventional six-switch full-bridge converter.

B. CASE 4 vs. CASE 2

The proposed DCM SEPIC rectifier with MPPA control strategy has higher power factor value compared to the DCM BOOST with conventional PFC. Implementation of the converter of case 4 has lower cost than case 2. In addition, the input current of DCM BOOST has discontinuous waveform, which results in a higher peak current compared to the DCM SEPIC. It could be harmful to the generator windings. As can be seen in Table 4, the THD value for the input current of the proposed converter (8.5%) is much lower than that of the DCM BOOST, which shows that the DCM SEPIC is a better choice for the PMSG power interface application than DCM BOOST.

C. CASE 4 vs. CASE 3

The same topology is used for both cases. Using the new MPPA control strategy instead of conventional one improves the performance in case 4. Comparing the performance of the converters, one can find the following advantages for the proposed control method:

1) Higher power factor: Using MPPA control strategy, a high power factor value obtained from the view point of the internal voltage source which results in lower generator current and less power loss.

2) Lower cost: One of the advantages of using the MPPA method is removing the input inductance of the DCM SEPIC and using the generator internal inductance alternately, which reduces volume and cost of the converter. As can be seen in Table 4, the cost of main components of the proposed converter is comparable to that of the conventional DCM Boost rectifier and is less than the active front end and the conventional SEPIC PFC rectifier. In addition, the proposed SEPIC converter has dimensions similar to the Boost converter, which are lower than those of the full-bridge converter. Therefore, it can be stated that the proposed converter has acceptable power density.

VII. CONCLUSION

In this paper, a simple low-cost DCM SEPIC with high input power factor was proposed for a small PMSG-based wind turbine generator system. A maximum power per ampere strategy was utilized, which uses the PMSG internal voltage as the power factor correction target point and PMSG phase inductances as the converter input inductances. By using the proposed method for the tested 500W PMSG, the generator current at rated power was reduced by 3.5% compared to the conventional PFC method and consequently the PMSG conductive loss was decreased by 7.1%.

Exploiting simple control system, single-switch structure with continuous input current, soft switching, and elimination of the input inductor, makes the proposed DCM SEPIC an efficient low-cost solution for rooftop wind turbines. In this regard, a small PMSG wind generator equipped with the proposed DCM SEPIC was theoretically analyzed, simulated, and prototyped in this paper.

REFERENCES

- [1] EA. *Tracking Power*. International Energy Agency. Paris, France, Accessed: Apr. 2020, Available: <https://www.ica.org/reports/tracking-power-2019>
- [2] Z. Chen, J. M. Guerrero, and F. Blaabjerg, "A review of the state of the art of power electronics for wind turbines," *IEEE Trans. Power Electron.*, vol. 24, no. 8, pp. 1859–1875, Aug. 2009.
- [3] M. Alemi-Rostami, G. Rezaadeh, R. Alipour-Sarabi, and F. Tahami, "Design and optimization of a large-scale permanent magnet synchronous generator," *Scientia Iranica*, to be published. [Online]. Available: http://scientiairanica.sharif.edu/article_21561.html
- [4] H. Polinder, F. F. A. van der Pijl, G.-J. de Vilder, and P. J. Tavner, "Comparison of direct-drive and geared generator concepts for wind turbines," *IEEE Trans. Energy Convers.*, vol. 21, no. 3, pp. 725–733, Sep. 2006.
- [5] W. Gul, Q. Gao, and W. Lenwari, "Optimal design of a 5-MW double-stator single-rotor PMSG for offshore direct drive wind turbines," *IEEE Trans. Ind. Appl.*, vol. 56, no. 1, pp. 216–225, Jan. 2020.
- [6] S. Jia, R. Qu, J. Li, X. Fan, and M. Zhang, "Study of direct-drive permanent-magnet synchronous generators with solid rotor back iron and different windings," *IEEE Trans. Ind. Appl.*, vol. 52, no. 2, pp. 1369–1379, Apr. 2016.
- [7] R. I. Putri, M. Pujiantara, A. Priyadi, T. Ise, and M. H. Purnomo, "Maximum power extraction improvement using sensorless controller based on adaptive perturb and observe algorithm for PMSG wind turbine application," *IET Electr. Power Appl.*, vol. 12, no. 4, pp. 455–462, Apr. 2018.
- [8] J. C. Y. Hui, A. Bakshai, and P. K. Jain, "An energy management scheme with power limit capability and an adaptive maximum power point tracking for small standalone PMSG wind energy systems," *IEEE Trans. Power Electron.*, vol. 31, no. 7, pp. 4861–4875, Jul. 2016.
- [9] G. Rezaadeh, F. Tahami, and H. Valipour, "Three-phase PFC rectifier with high efficiency and low cost for small PM synchronous wind generators," in *Proc. 7th Power Electron. Drive Syst. Technol. Conf. (PEDSTC)*, Feb. 2016, pp. 302–307.
- [10] Q. Deltenre, T. De Troyer, and M. C. Runacres, "Techno-economic comparison of rooftop-mounted PVs and small wind turbines: A case study for Brussels," *IET Renew. Power Gener.*, vol. 13, no. 16, pp. 3142–3150, Dec. 2019.
- [11] S. Zhang, K.-J. Tseng, D. M. Vilathgamuwa, T. D. Nguyen, and X.-Y. Wang, "Design of a robust grid interface system for PMSG-based wind turbine generators," *IEEE Trans. Ind. Electron.*, vol. 58, no. 1, pp. 316–328, Jan. 2011.
- [12] A. Tajfar, H. Riazmontazer, and S. K. Mazumder, "Harmonics analysis for a high-frequency-link (HFL) inverter," in *Proc. IEEE Energy Convers. Congr. Expo. (ECCCE)*, Sep. 2014, pp. 2335–2341.
- [13] J. W. Kolar and T. Friedli, "The essence of three-phase PFC rectifier systems—Part I," *IEEE Trans. Power Electron.*, vol. 28, no. 1, pp. 176–198, Jan. 2013.
- [14] T. Friedli, M. Hartmann, and J. W. Kolar, "The essence of three-phase PFC rectifier systems—Part II," *IEEE Trans. Power Electron.*, vol. 29, no. 2, pp. 543–560, Feb. 2014.
- [15] R. W. Erickson, *Fundamentals of Power Electronics*. New York, NY, USA: Springer, 2013.
- [16] E. H. Ismail, "Bridgeless SEPIC rectifier with unity power factor and reduced conduction losses," *IEEE Trans. Ind. Electron.*, vol. 56, no. 4, pp. 1147–1157, Apr. 2009.
- [17] Y. Jang and M. M. Jovanovic, "A new input-voltage feedforward harmonic-injection technique with nonlinear gain control for single-switch, three-phase, DCM boost rectifiers," *IEEE Trans. Power Electron.*, vol. 15, no. 2, pp. 268–273, Mar. 2000.
- [18] D. S. Lyrio Simonetti, J. Sebastian, and J. Uceda, "The discontinuous conduction mode Sepic and Cuk power factor preregulators: Analysis and design," *IEEE Trans. Ind. Electron.*, vol. 44, no. 5, pp. 630–637, Oct. 1997.
- [19] R. Foroozeshfar, E. Adib, and H. Farzanehfard, "New single-stage, single-switch, soft-switching three-phase SEPIC and Cuk-type power factor correction converters," *IET Power Electron.*, vol. 7, no. 7, pp. 1878–1885, Jul. 2014.
- [20] A. M. Al Gabri, A. A. Fardoun, and E. H. Ismail, "Bridgeless PFC-modified SEPIC rectifier with extended gain for universal input voltage applications," *IEEE Trans. Power Electron.*, vol. 30, no. 8, pp. 4272–4282, Aug. 2015.
- [21] G. Tibola and I. Barbi, "Isolated three-phase high power factor rectifier based on the SEPIC converter operating in discontinuous conduction mode," *IEEE Trans. Power Electron.*, vol. 28, no. 11, pp. 4962–4969, Nov. 2013.
- [22] A. Anand and B. Singh, "Power factor correction in Cuk–SEPIC-based dual-output-converter-fed SRM drive," *IEEE Trans. Ind. Electron.*, vol. 65, no. 2, pp. 1117–1127, Feb. 2018.
- [23] C. G. Bianchin, R. Gules, A. A. Badin, and E. F. R. Romaneli, "High-power-factor rectifier using the modified SEPIC converter operating in discontinuous conduction mode," *IEEE Trans. Power Electron.*, vol. 30, no. 8, pp. 4349–4364, Aug. 2015.
- [24] P. J. S. Costa, C. H. Illa Font, and T. B. Lazzarin, "A family of single-phase voltage-doubler high-power-factor SEPIC rectifiers operating in DCM," *IEEE Trans. Power Electron.*, vol. 32, no. 6, pp. 4279–4290, Jun. 2017.
- [25] A. J. Sabzali, E. H. Ismail, M. A. Al-Saffar, and A. A. Fardoun, "New bridgeless DCM sepic and cuk PFC rectifiers with low conduction and switching losses," *IEEE Trans. Ind. Appl.*, vol. 47, no. 2, pp. 873–881, Apr. 2011.
- [26] I. Yahyaoui, *Advances in Renewable Energies and Power Technologies: Solar and Wind Energies*, vol. 1. Amsterdam, The Netherlands: Elsevier, 2018.
- [27] D. Ochoa and S. Martinez, "Fast-frequency response provided by DFIG-wind turbines and its impact on the grid," *IEEE Trans. Power Syst.*, vol. 32, no. 5, pp. 4002–4011, Sep. 2017.



MEHDI ALEMI-ROSTAMI was born in Behashahr, Iran, in 1980. He received the B.Sc. degree in power electronics from Gilan University, Gilan, Iran, in 1998, and the M.S. and Ph.D. degrees in power electronics from Iran University of Science and Technology, Tehran, Iran, in 2000 and 2011, respectively. He is currently an Assistant Professor with Khayam Research Institute (KRI), Ministry of Science, Research, and Technology, Tehran.



GHASEM REZAADEH was born in Freydoonkenar, Iran, in 1990. He received the B.S. degree in electrical engineering from Shahid Beheshti University, in 2012, the M.Sc. degree from Sharif University of Technology, Tehran, Iran, in 2014, and the Ph.D. degree in a co-supervision in between Sharif University of Technology and the University of Picardie "Jules Verne," Amiens, France, in 2021. His research interests include electrical design and modeling electrical machine and power electronics converters.



FARZAD TAHAMI (Senior Member, IEEE) received the B.S. degree in electrical engineering from Ferdowsi University of Mashhad, Mashhad, Iran, in 1991, and the M.S. and Ph.D. degrees in electrical engineering from the University of Tehran, Tehran, Iran, in 1993 and 2003, respectively. From 1991 to 2004, he was with the Research and Development Department, Jovain Electrical Machines Corporation (JEMCO), Iran. In 2004, he joined Sharif University of Technology, Tehran, where he is currently an Associate Professor. Since 2007, he has been the Chairman of the technical committee of rotating machinery, The Iranian National Electrotechnical Committee (INEC). He is a member of the Board of Directors and the Chairman of the education committee of the Power Electronics Society of Iran (PESI).



MOHAMMAD HASAN RAVANJI (Member, IEEE) received the B.Sc., M.Sc., and Ph.D. degrees in electrical engineering from Sharif University of Technology, Tehran, Iran, in 2012, 2014, and 2020, respectively. His current research interests include renewable energy and design, optimization, and performance analysis of electrical machines.